

MULTI-VARIABLE DEMAND POWER PREDICTION FOR HEAVY-DUTY TRACTORS BASED ON MULTI-TASK LEARNING AND DYNAMIC WEIGHT OPTIMIZATION

ZHIJUN REN¹, YAN MA², FENGGANG LI³, YANMING FENG⁴, XINFAXU⁵, GUOWEI CAO⁶

Abstract

To improve the accuracy of power demand prediction for heavy-duty tractor trucks under complex working conditions, this study proposes a synchronous prediction model based on multi-task learning (MTL-A). This model innovatively synchronously predicts three key variables: vehicle speed, road slope, and acceleration, and takes driving style and road scenarios as labeled inputs to enhance the model's perception ability of complex working conditions. Firstly, a real vehicle data collection platform was established to obtain cumulative driving data of three drivers with distinct driving styles over more than 1800 kilometers in high-speed and national road scenarios. On this basis, the impact mechanism of each variable on power demand was quantitatively analyzed based on the vehicle longitudinal dynamics model, and the significant contributions of driving style and road conditions to power fluctuations were revealed. The proposed MTL-A model adopts the CNN-LSTM-Attention (CNN-LSTM-A) architecture and introduces the GradNorm algorithm to dynamically balance the loss weights in multi-task learning, thereby alleviating gradient conflicts and achieving

¹ State Key Laboratory of Engine and Powertrain System, Weichai Power Company Limited, China, email: renzj@weichai.com, ORCID: 0009-0000-5969-8237

² State Key Laboratory of Engine and Powertrain System, Weichai Power Company Limited, China, email: may@weichai.com, ORCID: 0009-0008-8918-434X

³ State Key Laboratory of Engine and Powertrain System, Weichai Power Company Limited, China, email: lifg@weichai.com, ORCID: 0009-0001-5916-7214

⁴ State Key Laboratory of Engine and Powertrain System, Weichai Power Company Limited, China, email: fengym@weichai.com, ORCID: 0009-0009-3461-0054

⁵ State Key Laboratory of Engine and Powertrain System, Weichai Power Company Limited, China, email: xuxinfa@weichai.com, ORCID: 0000-0001-8976-0396

⁶ State Key Laboratory of Engines, Tianjin University, China, email: cgw_123456@tju.edu.cn, ORCID: 0009-0000-2940-4226

precise multi-variable prediction in a short period. Experimental results show that compared with traditional single-task models, the average error of MTL-A model in predicting vehicle speed, slope, and acceleration is significantly reduced by 28.4%, 13.1%, and 16.3% respectively, thereby significantly improving the calculation accuracy of the final power demand. Particularly, in typical scenarios of high-speed and national roads, the power prediction error of MTL-A model is reduced by 58.40% and 41.68% respectively compared with traditional methods, fully verifying its excellent scene adaptability and prediction efficiency.

Keywords: multi-task learning; power demand prediction; CNN-LSTM-A architecture; GradNorm dynamic weight adjustment; scene adaptability

1. Introduction

As a crucial means of transportation and production tool, heavy-duty tractors play a vital role in improving logistics efficiency, supporting urban development, and ensuring the security of material supply. However, the rapid growth in the production and sales of heavy-duty tractors has also brought severe energy and environmental challenges. Under the “Dual Carbon” strategy, improving energy efficiency in heavy-duty tractors has become a key task for reducing carbon emissions and optimizing operational costs, with powertrain control being a core component.

Traditional vehicle powertrain control strategies typically rely on preset rules or decisions based on instantaneous information [1–3]. This control approach is inherently reactive and passive, exhibiting significant limitations in adaptability when confronted with the complex and dynamic traffic environments and operating conditions encountered in real-world driving scenarios. In recent years, predictive control has emerged as the mainstream technical approach for heavy-duty tractor powertrain control [4]. This is due to its ability to model and extrapolate future operational trends based on historical states, thereby enabling advance optimization of control strategies. Power demand prediction serves as the critical bridge linking control strategies to vehicle dynamic requirements, providing essential support for achieving predictive control objectives.

Indirect power demand prediction based on vehicle speed forecasting typically involves predicting future speed and acceleration and estimating power via vehicle dynamics models. These methods fall into two main categories. The first focuses solely on speed prediction: for instance, Xing et al. [5] combined CNN and LSTM to forecast vehicle speed for use in MPC-based energy management; Qifan Xue [6] used Informer FDR (Informer with fusion features, dilated causal convolution, and residual connection) to predict vehicle speed. The proposed model uses an improved encoder-decoder structure based on the Informer model; Chen et al. [7] proposed a fuzzy C-means clustering enhanced Markov Chain method to predict the leading vehicle's speed for fuel cell hybrid electric heavy trucks, and the predic-

tion results were applied to upper-layer speed planning to minimize the host vehicle's power demand and maintain a safe inter-vehicle distance.; Luca Pulvrenti [8] proposed an Adaptive V2X-connectivity-based Equivalent Consumption Minimization Strategy (A-V2X-ECMS), which leverages short-term vehicle speed prediction provided by Vehicle-to-Everything (V2X) connectivity, adopts Principal Component Analysis (PCA) to reduce the dimensionality of energetic indices for driving pattern recognition, and uses a Long Short-Term Memory (LSTM) deep learning model to adaptively determine the optimal equivalence factor of ECMS. Guo et al. [9] used an ARIMA model to predict both speed and road gradient, and validated the resulting control strategy's effectiveness; Zhang, Q et al. [10] proposed a real-time fuzzy learning algorithm (FLA) for Markov Chain (MC), which constructed the MC with vehicle velocity as the state based on the NGSIM highway traffic dataset. By adaptively updating the MC's transition probability matrix through FLA, the algorithm realized short-term vehicle speed prediction, achieving a root mean square error (RMSE) of only 0.82 m/s for the 1-second prediction horizon; Yue et al. [11] used different Markov chain models to forecast speed and gradient, with speed errors under 5.4 km/h over 5 seconds; Zhou Yang et al. [12] proposed a vehicle speed prediction method based on self-learning multi-step Markov chains. This method updates the transition probability matrix in real time through online measured data and introduces a forgetting factor to adapt to various working conditions. It does not require an offline training database and takes into account both accuracy and real-time practicality; Cao et al. [13] predicted speed and gradient using a neural network and achieved a power prediction error of 14.8 kW, demonstrating relatively high accuracy.

Although the aforementioned research has achieved significant progress, the existing power prediction models for heavy-duty trucks still have obvious limitations. Firstly, most models simply map the power demand to vehicle speed or historical data, generally ignoring the profound influence of different driving styles on the driver's acceleration intention and operation rhythm, resulting in the models being unable to accurately reflect the power dynamic changes caused by differences in driver behavior. Secondly, the common practice is to only predict vehicle speed and adopt static assumptions for road gradients. In complex and variable road conditions on national highways or unstructured roads, the real-time fluctuations of acceleration and slope are significant, and this simplified treatment will introduce large errors, thereby seriously undermining the accuracy of the final power calculation.

Regarding the above issues, the main content of this study is as follows:

Chapter 2 constructed a real vehicle data collection platform for heavy-duty towing trucks. It connected the vehicle bus recorder through the OBD interface and collected key parameters such as speed, torque, and slope at a frequency of 10 Hz. For three drivers with significantly different driving styles, over 1800 kilometers of driving data were accumulated under two typical working conditions (highway and national road), providing a multi-source data foundation for research.

Chapter 3 quantitatively analyzed the influence mechanism of power demand based on the longitudinal dynamics model: Differences in road scenarios led to a 26.40% increase in the standard deviation of power on the high-speed sections of the national road (excluding the influence of slope), while the analysis of driving styles revealed that the standard deviation of power change rate for the same driver fluctuated as high as 101.19% in different trips, confirming the need for dynamic identification of driving behavior characteristics.

Chapter 4 proposed the MTL-A multi-task learning model, which synchronously predicts vehicle speed, slope, and acceleration using the CNN-LSTM-A architecture: Through coupling spatiotemporal features through shared layers, the self-attention mechanism enhances the extraction of key information, and the GradNorm algorithm dynamically balances the loss weights of the three tasks; the model reduced the error in vehicle speed prediction within 5 seconds by 28.4% compared to the single-task model, and improved the prediction accuracy of slope and acceleration by more than 13%.

Chapter 5 verified the model's performance and extracted conclusions: MTL-A reduced the RMSE of power prediction in the high-speed scenario to 21.19 kW within 5 seconds, and the introduction of driving style labels reduced the error by an additional 38.22%; the synchronous three-variable prediction strategy broke through the accuracy bottleneck of traditional indirect methods and provided a feasible solution with an error of 35.56 kW for complex scenarios such as national roads.

2. Materials and Methods

The Materials and Methods section should encompass detailed information regarding the research plan, procedures, tools, and techniques employed for data collection and analysis. Accuracy, clarity, and transparency of information are crucial in this section as they enable readers to comprehend how the study was conducted and why the methods chosen by the authors are suitable for their research objectives.

2.1. Data Acquisition Platform

The vehicle data used in the research was sourced from a certain heavy-duty freight tractor produced by a cooperating enterprise. This vehicle is powered by a diesel engine, with a maximum output power of 410 kW. It is equipped with a 16-speed AMT gearbox and is also fitted with a slope sensor, which can measure real-time road slope information. Figure 1 shows the physical image of the test vehicle. The basic parameters of the vehicle are listed in Table 1.



Fig. 1. Experimental vehicle

Tab. 1. Basic vehicle parameters

Data Name	Value	Data Name	Value
Vehicle length	7.425 m	Gross vehicle mass	8.8 t
Vehicle width	2.5 m	Rated load capacity	40 t
Vehicle height	3.95 m	Front track width	2060 mm
Drive configuration	6×4	Rear track width	1875 mm

The vehicle's on-board diagnostic system (On-Board Diagnostics, OBD) interface is connected via an automotive bus recorder to enable real-time reading and storage of vehicle operation data, as shown in Figure 2.



Fig. 2. Vehicle bus data recorder

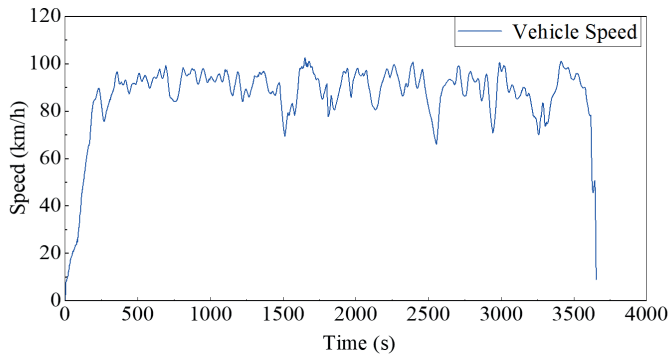
The data collection platform collects vehicle driving data at a frequency of 10 Hz. The obtained data include the vehicle's real-time driving speed, engine output torque, accelerator pedal opening degree, brake pedal opening degree, gear position, road slope, and other information. The specific data content is shown in Table 2.

Tab. 2. Primary Collected Data

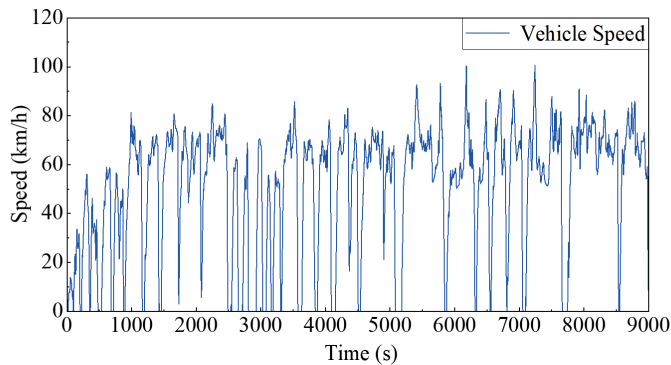
Column Name	Data Description	Unit
Vehicle_spd	Instantaneous vehicle speed	km/h
Torque	Engine output torque	N·m
Eng_spd	Engine speed	r/min
Slope_angle	Road slope angle	°
Pedal	Throttle pedal position	%
Brake	Brake pedal signal	0/1
Gear_num	Transmission gear position	-

2.2. Data Presentation

To reduce the influence of the vehicle itself and external environmental factors, the driving data of three drivers with different driving habits over a month were collected. Among them, there were 9 sets of data for the expressway route and 9 sets of data for the national road route, with a total mileage exceeding 1800 kilometers. The three drivers had significant differences in their driving habits, and had different requirements for the vehicle's power response and driving comfort, thus ensuring the diversity and balance of the sample data. The test routes were the common typical working conditions of heavy-duty freight tractor trucks, including the expressway and national road. The expressway route was 82 km long, with no traffic lights throughout the route, and the test vehicle could continuously drive on this section. The national road route was 128 km long, with several traffic lights along the route, and the working conditions were relatively complex, including both vehicle start-stop conditions caused by traffic lights and medium and low-speed conditions during normal driving. Figure 3 shows the information of the test routes.



[a] Highway Route



[b] National Road Route

Fig. 3. Raw speed curve of the test route

3. Analysis of Key Factors Affecting Power Demand

During the driving process, the power demand of the vehicle mainly stems from the longitudinal dynamic characteristics. The power output of the power system needs to not only compensate for the inertia power during the acceleration process but also overcome the power loss caused by the driving resistance [14]. In response to the real-time requirements of intelligent control under vehicle dynamic conditions, most existing studies adopt indirect prediction methods, that is, using the longitudinal speed as the prediction variable, and calculating the predicted power through the longitudinal driving dynamics [15], as shown in Equation (1).

$$P_t = P_a + P_f + P_{areo} + P_\theta = (mav + (Av + Bv^2 + Cv^3) + mgv \sin \theta)/3.6 \quad (1)$$

$$a = \frac{F_t - A - Bv - Cv^2 - mg \sin \theta}{m} \quad (2)$$

In the equation, P_t represents the total vehicle demand power, P_a represents the acceleration demand power, P_f represents the power required to overcome rolling resistance, P_{areo} represents the power required to overcome air resistance, and P_θ represents the power required to overcome slope resistance, m represents the vehicle mass, $A_v + B_v^2 + C_v^3$ represents the sum of rolling resistance and air resistance, where A , B , and C are the driving resistance coefficients obtained from the sliding test, and the unit of speed v is km/h. Acceleration a is calculated by equation (2), F_t represents the vehicle driving force, which can be obtained by calculating the engine output torque. Considering that in the case of coasting in neutral gear or braking, the vehicle does work against external resistance, at this time, no power needs to be output externally, therefore only the forward driving power is considered.

From equation (1), it can be seen that vehicle speed, road slope, and acceleration are the main time-varying variables affecting the calculation of demand power, while vehicle mass, driving resistance coefficients, etc., which are determined by measurement or experiment, can be regarded as known constants. Among them, vehicle speed is the basic variable of power demand, not only determining the size of air resistance, but also directly affecting the calculation result of power, thus reflecting the basic energy consumption required to maintain the vehicle's stable operation. Acceleration reflects the change in vehicle operating state, during acceleration, additional power input is required to overcome inertia, while during deceleration, the demand power decreases. Its change is not only related to traffic scenarios, but is also directly affected by driver behavior. Road slope as an external environmental factor significantly changes the forces acting on the vehicle along the longitudinal direction, thereby affecting the size of power demand. This effect is particularly obvious when the slope is large. The combined effect of these three factors determines the dynamic changes of instantaneous power.

In addition to vehicle speed, road slope, and acceleration, which are the direct variables necessary for calculating power by the dynamic formula, the vehicle demand power in practice is also affected by different road conditions and different driving styles of drivers. These two factors, as indirect variables affecting the demand power, cannot be ignored in the analysis of demand power.

3.1. Influence of Different Road Conditions on Power Demand

The driving performance of the test vehicle on highways and on national roads shows significant differences. The speed of the vehicle on national roads is significantly lower than that on highways. Comparing the average speed and the maximum speed, the national road section

has a reduction of 32.97% and 18.90% respectively compared to the highway section, while the average acceleration has increased by 111%, showing a considerable difference.

An analysis of the power performance differences on the two sections is conducted. In the forward drive power, the power required to overcome the slope resistance is excluded, and only the acceleration power during driving and the power required to overcome rolling resistance and air resistance are considered. The calculation is shown in Equation (3).

$$P_a + P_f + P_{areo} = P_t - P_\theta \quad (3)$$

In the equation, P_t represents the total vehicle driving power, P_a represents the acceleration demand power, P_f represents the power required to overcome rolling resistance, P_{areo} represents the power required to overcome air resistance, and P_θ represents the power required to overcome slope resistance.

As shown in Table 3, the comparison after removing the power required to overcome slope resistance is presented. It can be seen that on national roads, compared to expressways, the average power has decreased by 25.09%, the power standard deviation has increased by 26.40%, and the power fluctuation has become larger. By comparing the Q1-Q3 distribution ranges of power and power change rates, it can be observed that compared to expressways, national roads have increased by 29.23% and 23.68% respectively in terms of the distribution range of power and power change rates. Compared to the overall power distribution before removing the slope power, the gap in the distribution range of power change rates has decreased.

3.2. Influence of Driving Style on Power Demand

The driving styles of different drivers vary significantly, which leads to different power requirements for the entire vehicle. As shown in Table 3, it presents the comparison of the vehicle's demand power for the same road section but with different drivers. From the Q1 to Q3 distribution range of power and its rate of change, it can be seen that the power distribution range of driver A is the largest, increasing by 41.29% compared to driver B and 31.36% compared to driver C; driver B has the most concentrated power distribution range; and driver C has the largest change in power distribution range during the three trips, with the maximum difference being 47.65%. Among them, the power Q1 of driver A during the second and third trips was both 0, because it had more coasting operations, causing the demand power values to be concentrated around 0. The distribution range of the power change rate of the three drivers also varies, and the fluctuation of the power change rate of driver B is more stable.

Tab. 3. Comparison of power demand between different drivers

Driver	Test Group	Power Q1~Q3 [kW]	Power Rate of Change Q1~Q3 [kW/s]	Average Power [kW]	Power Std. Dev. [kW]	Power Rate of Change Std. Dev. [kW/s]
A	A1	14.58-178.63	-1.62-1.88	113.79	89.97	21.13
	A2	0.00-169.77	-1.56-1.64	102.60	87.35	22.07
	A3	0.00-175.11	-0.91-1.06	109.94	94.78	22.31
B	B1	45.69-174.17	-0.84-1.71	116.78	79.51	16.69
	B2	29.35-157.85	-1.33-1.82	106.37	77.42	14.32
	B3	67.80-171.01	-1.16-1.67	116.64	75.95	15.73
C	C1	44.50-195.12	-3.05-4.46	128.40	95.06	30.24
	C2	47.93-149.94	-0.97-2.23	105.22	77.24	17.78
	C3	16.46-151.27	-0.41-1.78	95.97	82.45	15.03

From this, it can be seen that the power requirements for different drivers can vary significantly. When the same road is driven by different drivers, the standard deviation of power and the standard deviation of power change rate can differ by up to 17.44% and 28.63% respectively for more aggressive drivers compared to more moderate drivers, showing a considerable difference. Moreover, the same driver may also vary in different external environments, with the average power, power standard deviation, and power change rate standard deviation of driver C potentially differing by 33.79%, 23.07%, and 101.19% respectively, indicating unstable driving performance. Therefore, using fixed labels to describe individual drivers is not advisable in practical applications.

In conclusion, in the analysis and prediction of power requirements, the driving style of drivers is an important variable. However, drivers and driving styles cannot be simply bound together because driving styles are variable and the influence of driving styles is also variable. In different driving scenarios, the same driver may exhibit different driving styles. When predicting power requirements, it is necessary to identify the current driving style of the driver and use it as the basic information for prediction.

4. Multi-Task Learning-Based Joint Prediction Model for Vehicle Speed, Acceleration, and Road Gradient

To address the issue of simultaneously predicting vehicle speed, acceleration, and road slope required for demand power prediction, a multi-task learning model MTL-A based on CNN-LSTM-A was proposed, which is used to predict the three variables of vehicle speed, acceleration, and road slope simultaneously.

Multi-Task Learning (MTL) is a deep learning method that enables a neural network to learn multiple tasks simultaneously, which can couple the intrinsic connections among the tasks and improve the overall learning effect [16].

When predicting the future short-term vehicle speed, acceleration, and road slope, the parameter sharing mechanism of MTL can capture and learn the correlations among various tasks. This indicates that when making predictions for the current task, the MTL model not only references historical data information but also utilizes the relevant information of the current trend changes of other tasks, thereby improving the prediction performance. In MTL, the overall loss function of the model can be obtained by weighting and summing the loss functions of each sub-task, and the calculation equation is as follows:

$$Loss_{MTL} = \sum_{i=1}^n c_i loss_i \quad (4)$$

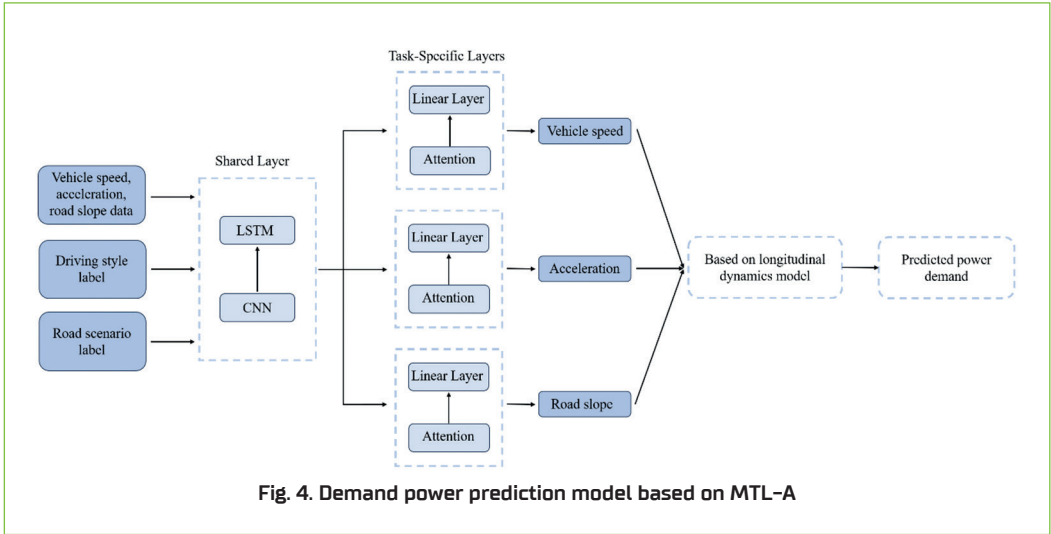
In Equation (4), $Loss_{MTL}$ represents the overall loss function of the model, $loss_i$ represents the loss function of each sub-task, and c_i represents the weight of the loss function.

In multi-task learning, the type of the shared layer of the network plays a crucial role in the prediction of the entire model. Since vehicle speed, acceleration, and road slope all have significant time series characteristics and the data at adjacent moments are highly correlated, considering the historical changes is crucial for the prediction of the three parameters. To better capture the temporal dependence of the input data, CNN-LSTM is selected as the shared layer of MTL. CNN can effectively extract local features, especially performing well in processing data with spatial structure. Combined with LSTM, CNN can first extract the local features of vehicle speed, acceleration, and slope data, and then capture the sequence dependencies over a long time range through LSTM. In this way, the CNN-LSTM model not only can extract key local features but also can effectively handle input data with a long time span, which is helpful for improving the prediction performance of the overall model.

To fully combine the feature extraction ability of CNN-LSTM and the ability of Multi-head Self-Attention to obtain the global patterns and dependencies of the sequence, a multi-task learning model structure named CNN-LSTM-A, i.e., MTL-A model, is proposed. In the shared layer of CNN-LSTM, it can effectively extract the local features of the time series and capture the sequence dependencies over a long time range, while the self-attention mechanism helps the model focus more on the time steps or feature dimensions that have a greater impact on the prediction task. Therefore, the self-attention layer is placed in the specific task layer of each sub-task. Considering the influence of model accuracy and complexity, the adopted self-attention is a single-layer single-head attention structure.

The proposed joint prediction model structure for vehicle speed, acceleration, and road slope based on MTL-A is shown in Figure 4. The model's input is vehicle speed, acceleration, road slope data, as well as driving style labels and road scene labels. The road scene labels are

determined by an artificial annotation method and are used to distinguish whether the road belongs to a high-speed condition or a national road condition. The driver labels are provided in real time by the hierarchical Bayesian modeling method [17].



4.1. Model Parameter Selection

Selecting vehicle speed, acceleration, road slope, driver style labels, and road scene labels as inputs, and using future short-term vehicle speed, acceleration, and road slope as outputs, an MTL-A prediction model is constructed. To build the training set, the input and output features are processed using a sliding window approach, and the total length of the sliding window is determined by the length of historical data and the prediction time step. For example, when using 10 seconds of historical data to predict the output for the next 5 seconds, the sliding window size is 15, meaning the first 10 seconds of historical data are used as input samples, and the subsequent 5 seconds of data are used as regression targets. During the data sampling process, the sliding window moves one time step to the right each time to obtain new input samples and corresponding output targets.

The numerical ranges of different variables in the dataset vary greatly. For instance, vehicle speed is within the range of [0, 100] km/h, while the slope is within the range of [-3, 3]°. If the data is directly input into the neural network, variables with smaller values may be ignored, affecting the model's performance. Therefore, the data is normalized, and the normalization equation is as shown in [5].

$$X_i = \frac{x_i - x_{min}}{x_{max} - x_{min}}, i = 1,2,3, \dots, n \tag{5}$$

In multi-task learning networks, the structure design of the shared layer is crucial for feature extraction. This study, based on the characteristics of time series data, determines that the shared layer consists of a hybrid architecture combining convolutional neural networks and long short-term memory networks. The shared layer specifically consists of two one-dimensional convolutional layers connected with an LSTM layer. The 1D-CNN can efficiently extract local temporal features and patterns in the input sequence, while the subsequent LSTM layer is good at capturing long-term temporal dependencies in the sequence. The LSTM layer adopts a single hidden layer structure, with the number of hidden layer neurons set to 100 to balance model complexity and expressiveness. After this shared feature extraction layer, the network branches into three independent sub-task output layers, corresponding to the prediction of vehicle speed, slope, and acceleration. In terms of model training configuration, the loss function uses the mean absolute error as the base loss for each task. The dataset is randomly divided into training and test sets in a 7:3 ratio. The model training optimizer selects the adaptive moment estimation algorithm, with the learning rate set to 0.005. The entire training process consists of 150 rounds to ensure the model converges fully.

4.2. Total Loss Function Selection in MTL

The total loss function in multi-task learning is the weighted sum of the loss functions of individual tasks, as shown in Equation [4-3]. However, assigning fixed weights to tasks is not reasonable, as it can lead to unbalanced task optimization. For example, differences in gradient magnitude may cause inconsistent learning rates or dominant tasks overwhelming secondary ones. In addition, conflicting task objectives can result in gradient cancellation, and manually tuning task weights can be highly time-consuming.

To avoid the drawbacks of linear weighting, the Gradient Normalization (GradNorm) method is adopted to dynamically adjust loss weights. Its goal is to keep the loss gradients of different tasks balanced during training, preventing any task from dominating or being neglected[18]. The core idea is to dynamically adjust the weights of different tasks by normalizing their gradient norms, ensuring that all tasks learn at a similar rate.

Assuming there are T tasks in the MTL model, and the loss of each task is $L_i(i \in 1, 2, \dots, T)$, GradNorm dynamically adjusts the task weights w_i through the following steps:

Compute the gradient norm G_i of each task loss with respect to the shared network parameters θ_s .

$$G_i = \|\nabla_{\theta_s}(w_i L_i)\|_2 \quad (6)$$

Compute the mean of the gradient norms to measure the overall gradient magnitude.

$$\bar{G} = \frac{1}{T} \sum_{i=1}^T G_i \quad (7)$$

Compute the relative learning rate r_i of each task and the target gradient ratio \tilde{G}_i .

$$r_i = \frac{L_i(t)}{L_i(0)} \quad (8)$$

where $L_i(t)$ is the current loss of task i , and $L_i(0)$ is the initial loss of task i at the start of training.

$$\bar{r} = \frac{1}{T} \sum_{i=1}^T r_i \quad (9)$$

$$\tilde{G}_i = \bar{G} \times \left(\frac{r_i}{\bar{r}}\right)^\alpha \quad (10)$$

where α is a hyperparameter used to adjust the balance between tasks.

Compute the GradNorm loss.

$$L_{GradNorm} = \sum_{i=1}^T |G_i - \tilde{G}_i| \quad (11)$$

Update the task weights w_i .

$$\frac{d}{dt} \log w_i = -\lambda \frac{\partial L_{GradNorm}}{\partial w_i} \quad (12)$$

4.3. Comparison of Prediction Performance Across Different Models

To verify the predictive performance of the model, the developed joint prediction model of vehicle speed, acceleration and road slope was compared with the traditional power prediction model that only predicts the vehicle speed as a single variable. The accuracy of power prediction under different methods was compared. At the same time, considering the influence of the attention mechanism, the MTL model without the attention mechanism was also used as a comparison model. To eliminate the influence caused by the differences in the basic network types, the single-task vehicle speed prediction model adopted the CNN-LSTM structure. The MTL and MTL-A structures were the same but without the attention mechanism. The number of hidden layers, the number of neurons and the hyperparameters in the training process of the comparison models were determined empirically. The input features and MTL-A were the same.

Tab. 4. Comparison of RMSE for vehicle speed prediction errors

Road Type	Prediction Horizon [s]	Prediction Error RMSE [km/h]		
		CNN-LSTM	MTL	MTL-A
Highway	1	0.69	0.56	0.48
	3	1.35	1.28	1.09
	5	1.74	1.53	1.45
National Road	1	0.88	0.75	0.68
	3	1.47	1.36	1.14
	5	1.90	1.72	1.53

Table 4 presents the speed prediction error indicators of MTL-A and the comparison model on two driving routes. From the data in the table, it can be seen that in different scenarios and different prediction durations, the MTL-A prediction model has a better performance. The average prediction accuracy is 13.6% and 28.4% higher than that of MTL and CNN-LSTM, respectively. Compared with the general single-task speed prediction model, the MTL-A model adds slope and acceleration prediction simultaneously. This is due to the parameter sharing mechanism of multi-task learning. The interaction of tasks in the prediction can obtain some features that are difficult to capture normally, thus improving the prediction effect of sub-tasks.

Tab. 5. Comparison of RMSE for road slope prediction errors

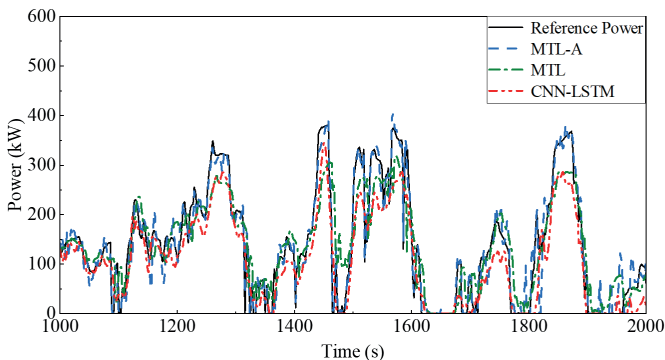
Road Type	Prediction Horizon [s]	Prediction Error RMSE [°]	
		MTL	MTL-A
Highway	1	0.059	0.051
	3	0.093	0.085
	5	0.145	0.132
National Road	1	0.078	0.067
	3	0.113	0.098
	5	0.182	0.163

Tab. 6. Comparison of RMSE for acceleration prediction errors

Road Type	Prediction Horizon [s]	Prediction Error RMSE [m/s ²]	
		MTL	MTL-A
Highway	1	0.021	0.019
	3	0.040	0.037
	5	0.053	0.044
National Road	1	0.037	0.028
	3	0.045	0.039
	5	0.069	0.062

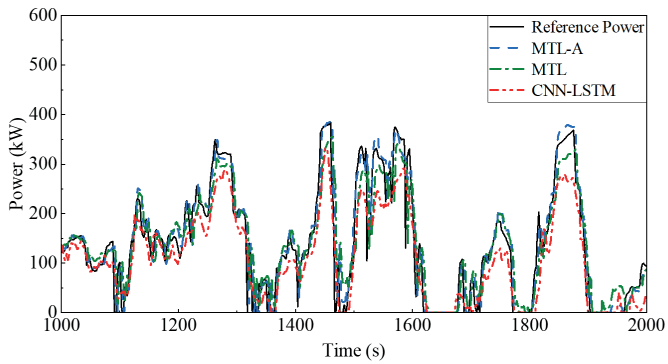
Tables 5 and 6 show the slope and acceleration prediction errors of the proposed MTL-A model and the MTL model on the dataset. The evaluation index adopted is the average value of RMSE calculated by comparing all single prediction results within the prediction time domain with the actual values. It can be seen from these that the MTL-A model maintains a high prediction accuracy for vehicle speed while also having good prediction effects for road slope and acceleration. Compared with MTL, the average prediction accuracy has increased by 13.1% and 16.3% respectively. The MTL-A model with the added attention mechanism has improved the prediction accuracy, enhancing the model's prediction effect.

Based on the predicted vehicle speed and corresponding road slope and acceleration obtained from the above models, the short-term predicted power is calculated using Equation (3-1). To fully verify the comparison effect, the CNN-LSTM comparison model calculates the short-term predicted power based on the predicted vehicle speed. The predicted acceleration is obtained by differentiating the predicted vehicle speed, and the road slope is assumed to be known in the future. The predicted power results are shown in Figures 5 and 6. The reference power is calculated based on the actual vehicle speed, road slope, and acceleration. To clearly and intuitively display the data characteristics and facilitate subsequent analysis and observation, for high-speed and national roadways, data with a duration of 1000 seconds are selected for visualization.

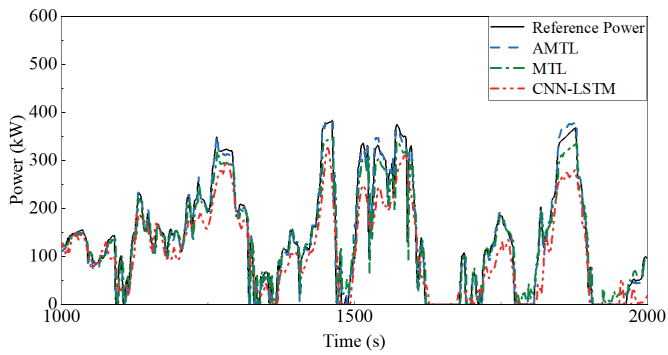


[a] Prediction Horizon: 5 seconds

Fig. 5. Power prediction results across multiple time horizons on highways

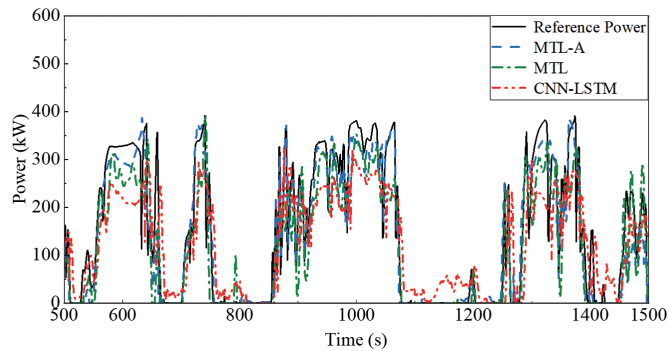


(b) Prediction Horizon: 3 seconds



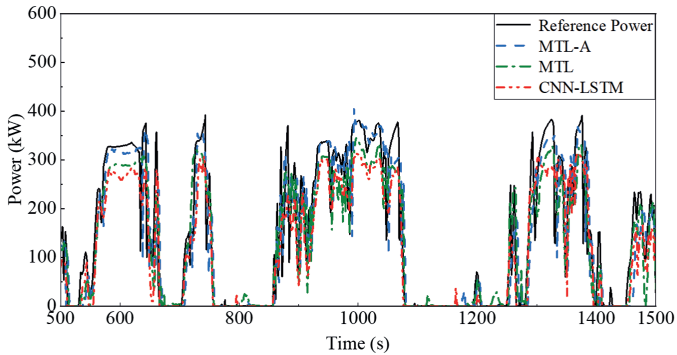
(c) Prediction Horizon: 1 second

Fig. 5. Power prediction results across multiple time horizons on highways; cont.

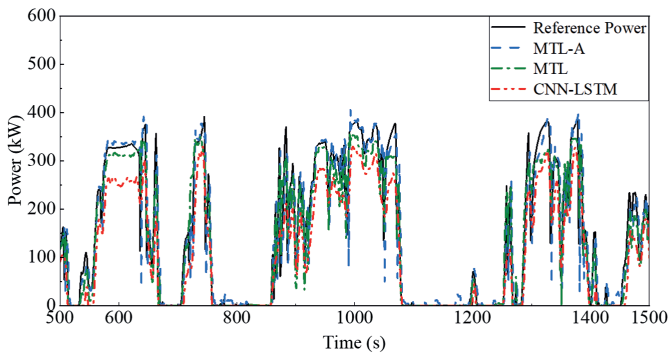


(a) Prediction Horizon: 5 seconds

Fig. 6. Power prediction results across multiple time horizons on national roads



[b] Prediction Horizon: 3 seconds



[c] Prediction Horizon: 1 second

Fig. 6. Power prediction results across multiple time horizons on national roads; cont.

From Figures 5 and 6, it can be seen that under the same prediction duration, compared with the CNN-LSTM model that only predicts vehicle speed, the MTL-A model and MTL model that simultaneously predict vehicle speed, slope, and acceleration have better performance in the prediction of the vehicle's demand power, and better track the trend of actual power changes. From the two different scenarios of high-speed and national highways, in the high-speed scenario, the vehicle speed is relatively stable and the power change fluctuation is smaller. The power prediction accuracy of the MTL-A prediction model in this scenario is higher; while in contrast, the national highway scenario is complex, with fast changes in vehicle speed and power, which leads to larger power prediction errors of the prediction model in this scenario and poorer prediction effect compared to the high-speed scenario. As the prediction duration increases, the prediction model inevitably has a certain decrease in accuracy, which is reflected in the figure as the local spikes and sudden changes in power at 5 seconds being larger. Table 7 shows the calculated short-term power prediction errors.

Tab. 7. Comparison of RMSE for power prediction errors

Road Type	Prediction Horizon [s]	Prediction Error RMSE [kW]		
		CNN-LSTM	MTL	MTL-A
Highway	1	38.37	25.12	13.32
	3	44.41	30.78	19.70
	5	47.53	34.59	21.19
National Road	1	47.82	35.86	22.64
	3	49.99	39.64	29.47
	5	52.51	46.23	35.56

As can be seen from Table 7, under the same prediction duration, the demand power error predicted by the MTL-A model is significantly smaller than that predicted by the CNN-LSTM and MTL models. The CNN-LSTM model only predicts the vehicle speed but does not predict the corresponding acceleration. Thus, the predicted acceleration based on the difference in vehicle speed and the reference acceleration will be different, which will cause an increase in the calculation power error. However, the MTL-A model simultaneously considers the prediction of vehicle speed, road slope, and acceleration, which is more in line with the actual situation, and therefore the demand power prediction error is also smaller. The power prediction error in the national road scenario is significantly higher than that in the expressway scenario. This is because the speed and acceleration changes in the national road scenario are complex and fluctuate greatly, which leads to intense power fluctuations and an increase in the prediction error.

In conclusion, the speed predicted by the speed-road slope-acceleration model based on MTL-A is more accurate than that predicted by the single-task CNN-LSTM model, and the MTL-A model also considers the prediction of road slope and acceleration. Thus, the predicted power demand values calculated through the dynamic equation are also more accurate.

5. Conclusions

[1] An experimental data acquisition platform was established based on heavy-duty diesel-powered tractor trucks, collecting driving data over one month from three drivers with distinct driving habits, totaling over 1,800 kilometers. By analyzing OBD-collected data such as vehicle speed and torque, patterns influencing the power consumption of heavy-duty tractor trucks were identified. The multi-task learning demand power prediction model MTL-A was developed. This model comprehensively considers road gradient and driver style to predict demand power under highway and national road conditions.

- [2] Analysis of power demand for the same driver across different road scenarios revealed significant road condition impacts, necessitating scenario-specific considerations in power demand forecasting. Specifically: Average total power across all sections decreased by 25.09% on national highways compared to expressways, while power standard deviation increased by 26.40%. The interquartile ranges (Q1–Q3) for power and power variability increased by 29.23% and 23.68%, respectively, indicating more pronounced power fluctuations on national highways. Comparing stable driving segments between national highways and expressways, average power on national highways decreased by 44.12%, while acceleration-related power demand increased by 38.05%, highlighting the greater influence of individual driving behavior on power consumption. During stationary acceleration at national highway intersections, average power exceeded highway acceleration start-up by 17.60%, with the Q3 value of power variation rate reaching 2.66 times that of highway start-up, reflecting higher power demand and more intense fluctuations.
- [3] Developed the Multi-Task Learning Power Demand Prediction Model MTL-A, capable of simultaneously predicting vehicle speed, road gradient, and acceleration. This model incorporates traffic scenarios and driving styles as independent classification variables into its input. By applying predictive variables within longitudinal dynamic equations, it achieves more precise power demand forecasting. Specifically, in highway and national highway test scenarios, integrating driving style information reduced power prediction errors by 38.22% and 23.30%, respectively, significantly enhancing model accuracy. Furthermore, under both highway and national highway conditions, the MTL-A model—which simultaneously predicts vehicle speed, gradient, and acceleration—reduced power prediction errors by 58.40% and 41.68%, respectively, compared to the CNN-LSTM model that only predicts vehicle speed. Regarding vehicle speed prediction, the MTL-A model achieved over 19% lower error than the CNN-LSTM baseline model.

6. Acknowledgement

This work is supported by the Taishan Industrial Experts Program.

7. Nomenclature

V2X	Vehicle-to-Everything
EMS	Energy Management System
MPC	Model Predictive Control
ECMS	Equivalent Consumption Minimization Strategy
LSTM	Long Short-Term Memory
AMT	Automated Manual Transmission
RMSE	Root Mean Squared Error

OBD	On-Board Diagnostics
GPS	Global Positioning System
PCA	Principal components analysis
MTL	Multi-task learning
GradNorm	Gradient Normalization

References

- [1] Fan Y, Peng J, Yu S, Yan F, Wang Z, Li M, et al. Global optimization guided energy management strategy for hybrid electric vehicles based on generative adversarial network embedded reinforcement learning. *Energy*. 2025;322:135586. <https://doi.org/10.1016/j.energy.2025.135586>.
- [2] Chen D, Chen T, Li Z, Liu Z, Sun C, Zhao H. Energy management strategy for plug-in hybrid electric vehicles based on vehicle speed prediction and limited traffic information. *Energy*. 2025;136292. <https://doi.org/10.1016/j.energy.2025.136292>.
- [3] Dawei M, Yu Z, Meilan Z, Risha N. Intelligent fuzzy energy management research for a uniaxial parallel hybrid electric vehicle. *Computers & Electrical Engineering*. 2017;58:447–464. <https://doi.org/10.1016/j.compeleceng.2016.03.014>.
- [4] Zhang F, Hu X, Langari R, Cao D. Energy management strategies of connected HEVs and PHEVs: Recent progress and outlook. *Progress in Energy and Combustion Science*. 2019;73:235–256. <https://doi.org/10.1016/j.pecs.2019.04.002>.
- [5] Xing J, Chu L, Hou Z, Sun W, Zhang Y. Energy management strategy based on a novel speed prediction method. *Sensors*. 2021;21(24):8273. <https://doi.org/10.3390/s21248273>.
- [6] Xue Q, Ma J, Zhao X, Liu R, Li H, Zhu X. Informer-FDR: A short-term vehicle speed prediction model in car-following scenario based on traffic environment. *Expert Systems with Applications*. 2025;262:125655. <https://doi.org/10.1016/j.eswa.2024.125655>.
- [7] Chen B, Ma R, Zhou Y, Ma R, Jiang W, Yang F. Co-optimization of speed planning and cost-optimal energy management for fuel cell trucks under vehicle-following scenarios. *Energy Conversion and Management*. 2024;300:117914. <https://doi.org/10.1016/j.enconman.2023.117914>.
- [8] Pulvirenti L, Rolando L, Millo F. Energy management system optimization based on an LSTM deep learning model using vehicle speed prediction. *Transportation Engineering*. 2023;11:100160. <https://doi.org/10.1016/j.treng.2023.100160>.
- [9] Guo J, He H, Sun C. ARIMA-based road gradient and vehicle velocity prediction for hybrid electric vehicle energy management. *IEEE Transactions on Vehicular Technology*. 2019;68(6):5309–5320. <https://doi.org/10.1109/TVT.2019.2912893>.
- [10] Zhang Q, Filev D, Szwabowski S, Langari R. A real-time fuzzy learning algorithm for Markov chain and its application on prediction of vehicle speed. 2019 IEEE International Conference on Fuzzy Systems (FUZZ-IEEE), 2019 June 23–26. New Orleans, LA, USA. <https://doi.org/10.1109/FUZZ-IEEE.2019.8858893>.
- [11] Yue F, Liu Q, Kong Y, Zhang J, Xu N. A predictive energy management strategy for multi-energy source vehicles based on full-factor trip information. *Sensors*. 2022;22(1):23. <https://doi.org/10.3390/s22010023>.
- [12] Zhou Y, Ravey A, Pera MC. A velocity prediction method based on self-learning multi-step Markov chain. *IECON 2019–45th Annual Conference of the IEEE Industrial Electronics Society* 2019;1:2598–2603. <https://doi.org/10.1109/IECON.2019.8927191>.
- [13] Cao Y, Liang C, Cheng S, Yin X, Chen D, Liu Z, et al. Predictive Energy Management Strategy for Heavy-Duty Series Hybrid Electric Vehicles Based on Drive Power Prediction. *World Electric Vehicle Journal*. 2025;16(3). <https://doi.org/10.3390/wevj16030186>.

-
- [14] Pang Z, Zhang J, Jiao X, Ren L. Energy management strategy combining double deep Q-networks and demand torque prediction for connected hybrid electric vehicles. *IEEJ Transactions on Electrical and Electronic Engineering*. 2024;19(2):234–246. <https://doi.org/10.1002/tee.23942>.
- [15] Feng J, Han Z, Wu Z, Li M. Approximate optimal energy management with a high-precision vehicle speed prediction algorithm. *Proceedings of the Institution of Mechanical Engineers, Part D: Journal of Automobile Engineering*. 2024;238(4):774–787. <https://doi.org/10.1177/09544070221134332>.
- [16] Wen M, Mei H, Yuan F. Survey of multi-task recommendation algorithms. *Journal of Frontiers of Computer Science and Technology*. 2024;2:363–377. <https://doi.org/10.3778/j.issn.1673-9418.2303014>.
- [17] Ping M, Yan WJ, Jia X, Papadimitriou C, Yuen KV. Learning non-stationary model of prediction errors with hierarchical Bayesian modeling. *Reliability Engineering & System Safety*. 2025;260:111012. <https://doi.org/10.1016/j.ress.2025.111012>.
- [18] Chen Z, Badrinarayanan V, Lee CY, Rabinovich A. Gradnorm: Gradient normalization for adaptive loss balancing in deep multitask networks. *Proceedings of the 35th International Conference on Machine Learning*. 2018;80:794–803. <https://doi.org/10.48550/arXiv.1711.02257>.